A population of $CD4^+$ T cells with a naïve phenotype stably polarized to the T_H1 lineage

Jonathan W. Lo[1], Maria Vila de Mucha[2], Luke B. Roberts[1], Natividad Garrido-Mesa[1], Arnulf Hertweck[2], Joana F. Neves[1], Emilie Stolarczyk[1], Stephen Henderson[2], Ian Jackson[1], Jane K. Howard[1], Richard G. Jenner[2*], Graham M. Lord[1,3,*]

[1]School of Immunology and Microbial Sciences, King's College London, London, SE1 9RT, United Kingdom

[2]UCL Cancer Institute and CRUK UCL Centre, University College London (UCL), 72 Huntley Street, London, W1T 4JF, United Kingdom

[3]Faculty of Biology, Medicine and Health, University of Manchester, Manchester, United Kingdom.

Corresponding Authors: r.jenner@ucl.ac.uk and graham.lord@manchester.ac.uk

Abstract

T-bet is the lineage-specifying transcription factor for $CD4^+$ T helper type 1 (T_H1) cells. T-bet has also been found in other $CD4^+$ T cell subsets, including T_H17 cells and T_{REG}, where it modulates their functional characteristics. However, we lack information on when and where T-bet is expressed during T cell differentiation and how this impacts T cell function. To address this, we traced the ontogeny of T-bet-expressing cells using a fluorescent fate-mapping mouse line. We demonstrate that T-bet is expressed in a subset of $CD4^+$ T cells with naïve cell surface markers and that this novel cell population is phenotypically and functionally distinct from conventional naïve $CD4^+$ T cells. These cells are also distinct from previously described populations of memory phenotype and stem cell-like T cells. Naïve-like T-bet-experienced cells are polarised to the T_H1 lineage, predisposed to produce IFNγ upon cell activation, and resist repolarisation to other lineages *in vitro* and *in vivo*. These results demonstrate that lineage-specifying factors can function to polarise T cells in the absence of canonical markers of T cell activation and that this has an impact on the subsequent T helper response.

Introduction

Upon encounter with specific antigen, naïve $CD4^+$ T cells differentiate into one of several T helper cell subtypes, including T_H1, T_H2, T_H17, follicular T cells (T_{FH}) and peripheral regulatory T cells (pT_{REG}). $CD4^+$ T cell fate depends on the cytokine environment, signalling through the T cell receptor (TCR), and the transcription factors that these induce. Differentiation of T_H1 cells is triggered in response to presentation of bacterial antigens by antigen presenting cells (APCs) [1] and requires IL-12-mediated activation of STAT4 [2]. T_H1 cells are characterised by their production of interferon gamma (IFNγ), which activates cell-mediated immunity against intracellular bacteria, viruses, and tumour cells. Inappropriate or excessive T_H1 responses also contribute to inflammatory diseases, highlighting the importance of understanding the regulation of T_H1 cell differentiation.

Differentiation of naïve T cells into T_H1 effectors requires the T-box transcription factor T-bet, encoded by *Tbx21*, which is upregulated via IL12-dependent activation of STAT4 [2, 3]. T-bet directly activates *Ifng*, and a number of other genes encoding cytokines and receptors, including *Il12rb2*, *Cxcr3* and *Ccl4* [2, 4-6]. T-bet also activates its own expression, by both directly binding to its own gene and via IFNγ-mediated activation of STAT1 [7, 8]. T-bet mediated *Ifng* activation is accompanied by chromatin modifications that are maintained in memory cells [9-11]. In addition to promoting T_H1 lineage-specification, T-bet also counteracts differentiation of $CD4^+$ T cells into other lineages. T-bet represses expression of the gene encoding the T_H2 lineage-specifying factor *Gata3* [12] and blocks GATA3 binding to its target genes [8, 13]. T-bet also supresses T_H17 differentiation by blocking upregulation of the genes encoding RORγt and IRF4 [14, 15].

Although serving as the T_H1 lineage-specifying transcription factor, under certain conditions T-bet can also be expressed in T_H2, T_H17, pT_{REG} and in a T_{FH}-T_H1 transitional state, revealing a level of plasticity in $CD4^+$ T cell differentiation [16, 17]. Functionally, T-bet expression in T_H17 cells is associated with disease in an allergic encephalomyelitis mouse model [18-20] and T-bet is required for T_{REG} homoeostasis and function during T_H1-mediated inflammation [21]. T-bet also plays key roles outside of $CD4^+$ T cells, including $CD8^+$ cytotoxic T cells, γδ

T cells, natural killer (NK) cells, natural killer T (NKT) cells, type I and type 3 innate lymphoid cells (ILCs), dendritic cells (DCs), monocytes and B cells [3].

Dysregulated T-bet function is associated with inflammatory disease. T-bet is upregulated in lamina propria T cells of patients with Crohn's and celiac disease and *ex vivo* culture of biopsies from untreated celiac patients with gliadin increases T-bet expression through STAT1 activation [22, 23]. Genetic variants associated with ulcerative colitis and Crohn's disease are enriched at T-bet binding sites and can alter T-bet binding to its target genes. Transfer of *Tbx21*$^{-/-}$ naïve CD4^{+} T cells into *Rag2*$^{-/-}$ mice gave rise to a higher proportion of IL-17A-producing CD4^{+} T cells and worse colitis compared to mice which received WT naïve CD4^{+} T cells [15, 24], suggesting that T-bet restrains in IL-17A-driven colitis in this model [24-27].

Naïve T cells can be identified by their surface markers and are generally defined as CD62L^{high} CD44^{low} CCR7^{high}. Consistent with their quiescent, non-antigen experienced state, naïve CD4^{+} T cells have not been found to contain T-bet [28, 29] or other lineage-specifying transcription factors, apart from GATA3, which is essential for CD4^{+} T cell homeostasis in addition to its role in T_H2 cell differentiation. In contrast, antigen-experienced central memory T cells (T_{CM}) and effector memory T cells (T_{EM}) are defined as CD62L^{high} CD44^{high} CCR7^{high} and CD62L^{low} CD44^{high} CCR7^{low}, respectively [30-33]. However, the distinction between naïve and memory cells is not always clear cut. Small numbers of memory-phenotype (MP) cells are found in normal, non-immunised mice [34-36]. MP cells, which are predominantly CD8^{+}, also arise in mice maintained under germ-free and antigen-free conditions and in humans before birth, indicating they develop in response to self-antigens [37, 38]. Within the MP cell population, virtual memory (VM) T cells (CD8^{+} CD62L^{low} CD44^{high} CD122^{high} CXCR3^{high} Ly6C^{high} CD49d^{low}) are highly proliferative and provide both antigen-specific immunity and exhibit bystander killing activity [37, 39, 40]. Memory T cells with a naïve phenotype (T_{MNP}) are a human CD8^{+} T cell population defined as CXCR3^{+} CD49d^{+} CCR7^{+} CD95^{lo} CD28^{int} and are also highly responsive [41]. T_H1-like memory phenotype (T_H1-like MP) T cells (CD4^{+} CD62L^{-} CD44^{+} CXCR3^{+} ICOS^{+} CD49d^{high}) have also been identified and have been found to help B cells produce antibodies and are rapidly able to produce T_H1 cytokines, like IFNγ, after stimulation with PMA and ionomycin [42]. Furthermore, they have been shown to express higher levels of T-bet [42]. Like naïve T cells, CD8^{+} T memory stem cells (T_{SCM}) are CD62L^{high} CD44^{low}

and exhibit high proliferative capacity, but co-express markers CD122 (IL-2Rβ), CXCR3, Sca-1, Bcl2 and low levels of T-bet [43-45]. A population of MP $CD4^+$ cells has also been identified [46, 47]. These cells are present in germ-free and antigen-experienced mice and develop from $CD5^{hi}$ naïve cells in the periphery in a TCR and CD28-dependent manner [46]. MP cells contain $T\text{-}bet^{lo}$, $T\text{-}bet^{int}$ and $T\text{-}bet^{hi}$ subpopulations, with $T\text{-}bet^{hi}$ MP cells providing a rapid, non-antigen specific, upregulation of IFNγ in response to infection [46].

Knowledge of the $CD4^+$ T cell subsets that express T-bet, the points during T cell ontogeny at which T-bet is expressed, and the impact of T-bet on cell function is important for understanding T cell differentiation and its dysregulation in disease. However, progress has been limited by our inability to identify cells that have experienced T-bet expression. To address this, we have developed a $T\text{-}bet^{cre}$ x $Rosa26\text{-}YFP^{fl\text{-}STOP\text{-}fl}$ mouse line in which YFP marks cells that have expressed T-bet during their ontogeny. Using this line, we report the discovery of a previously unobserved $CD4^+$ T cell population with a naïve cell surface phenotype, which, nevertheless, has experienced T-bet expression. Arising shortly after birth, these YFP^+ naïve $CD4^+$ T cells accounted for around 1% of splenic $CD4^+$ T cells and are distinct from previously identified populations of memory-like cells. Although displaying naïve cell surface markers, these T-bet-experienced cells were polarised towards the T_H1 lineage, predisposed to rapidly upregulate IFNγ upon activation, and stably maintained their phenotype in opposing polarisation conditions in vitro and in an *in vivo* colitis model. This work thus reveals a function for lineage-specifying transcription factors in polarisation of naïve-like $CD4^+$ T cells that shapes the subsequent immune response.

Materials and Methods

Animals

C56BL/6 *Rag1*$^{-/-}$ (Jackson labs) and *Rosa26*$^{YFP/+}$ (Jackson labs) mice were sourced commercially. *T-bet*$^{cre/+}$ mice were previously generated by our group. *T-bet*$^{cre/+}$ mice were bred with *Rosa26*$^{YFP/+}$ to generate the *T-bet*$^{cre/+}$ *Rosa26*$^{YFP/+}$ line (hereby referred to as T-bet^{FM} mice). The *T-bet*^{Amcyan} line was a kind gift obtained from Jinfang Zhu at NIH/NIAID (National Institute of Health-National Institute of Allergy and Infectious Diseases) in Maryland, USA. All mice used were aged between 6-12 weeks, unless stated otherwise. All animal experiments were performed in accredited facilities in accordance with the UK Animals (Scientific Procedures) Act 1986 (Home Office Licence Numbers PPL: 70/6792 and 70/8127).

Cell isolation and preparation

Adult mice were euthanized using an approved Schedule 1 method of inhalation of a rising concentration of carbon dioxide gas followed by cervical dislocation. Embryo and neonatal mice were euthanised by using an approved Schedule 1 method of decapitation. Spleen, thymus, liver, mesenteric lymph nodes (mLN), peripheral (axillary, inguinal and cervical) lymph nodes (pLN), colon and small intestines were excised and placed in cold phosphate buffered saline (PBS) solution.

Colon and small intestine lamina propria cells were isolated as described [48]. Small intestine and colon were cleaned, and faeces were removed. Afterwards, they were cut into 1-2 cm pieces using surgical scissors and put into 10 ml of Hank's balanced salt solution (HBSS) without Mg^{2+}/Ca^{2+} (Invitrogen) mixed with 5 mM EDTA and 10 mM HEPES (Fisher Scientific) and incubated at 37.5^{o}C with agitation for 20 mins. Next, intestinal pieces were filtered, and the subsequent intestinal pieces were sliced into fine pieces using scalpels and were collected in complete animal medium (RPMI (Gibco) with 10% heat-inactivated fetal calf serum (FCS) (Gibco,), 2 mM glutamine, 100 U/ml penicillin and 100 µg/ml streptomycin, HEPES (Fisher Scientific), non-essential amino acids, sodium pyruvate and 2-mercaptoethanol (Sigma). Collagenase (0.5 mg/ml, Roche), DNase (10 µg/ml, Roche) and dispase II (1.5 mg/ml, Roche) were added and the intestinal pieces incubated for a further 20 mins at 37°C with agitation. After incubation, the digestion mix was filtered once more and

centrifuged at 860g for 10 mins at 4°C. Intestinal lamina propria cells were collected at the interface after centrifugation through Percol and washed.

Splenic, thymus, liver, mLN and pLN cells were isolated into a single cell suspension in complete animal medium with the use of 70 µM mesh filter and general mechanical destruction. The suspension was centrifuged at 860g for 5 mins at 4°C and mLN and pLN. spleen, thymus and liver cell pellets resuspended, and red blood cells were lysed using a standard red blood lysis buffer (ACK). The liver pellet was then collected at the interface after centrifugation through Percol and washed.

Cell sorting

CD4^{+} cells were purified using LS positive selection magnetic-activated columns (MACs) and anti-CD4 (L3T4) beads (Miltenyi Biotec). CD4^{+} MACs sorted cells were further purified by fluorescence activated cell sorting using a FACS Aria (BD Biosciences) with a 70µm nozzle insert and FACS Diva software CD4^{+} MACs sorted cells were stained for 20 mins at 4°C in the dark with the following antibodies: anti-CD4-PerCPCy5.5 (RM4-5), anti-CD25-PE (PC61), anti-CD62L-PECy7 (MEL-14; Thermo Fisher) and anti-CD44-Pacific Blue (IM1.8.1; Thermo Fisher). Single positive compensation controls and unstained controls were used to set up instrument settings and for gating strategies. Cell purity was verified post-sort (requiring 95% purify) and cell viability assessed using trypan-blue staining.

Naïve T cell transfer model of colitis

Naïve T cells were transferred as described [26]. Spleens and mLNs were harvested from either WT C56/BL6 mice or T-bet^{FM} donor mice and mechanically disrupted, as described before. Naïve CD4^{+} T cells (CD4^{+} CD25^{-} CD44^{low} CD62L^{high}) were sorted using a FACS Aria to a purity of >95%, washed and resuspended in sterile PBS. *Rag2*$^{-/-}$ mice were injected intraperitoneally with 5 x 10^{5} naïve CD4^{+} cells per mouse, unless stated otherwise, and humanely culled after 6-8 weeks. Mice were monitored for their health every week for signs of illness.

Cell culture

Unfractionated single cell suspensions of splenocytes (2x10^{6}/ml), mLN (1x10^{6}/ml) and cLP cells (1x10^{6}/ml) were cultured in complete animal medium for 48 hours in a CO_2 controlled

incubator at 37°C and 5% CO_2. Sorted $CD4^+$ T cells were also cultured on pre-incubated anti-CD3/anti-CD28 bound plates in IL-2 (20ng/ml) (Sigma-Aldrich) for 2 days and then just IL-2 (20ng/ml) (Sigma-Aldrich) for a further 5 days.

$CD4^+$ T cell polarisation

Sorted $CD4^+$ T cells were cultured on anti-CD3/anti-CD28-bound plates for 2 days and specific cytokines added for either T_H0 (hIL-2 (20ng/ml)), T_H1 (anti-IL-4 (5µg/ml), mIL-12 (20ng/ml), hIL-2 (20ng/ml)), T_H2 (anti-IFNγ (20ng/ml), mIL-4 (20ng/ml), hIL-2 (20ng/ml)), T_H17 (anti-CD28 (5µg/ml), anti-IL-4 (5µg/ml), anti-IFNγ (20ng/ml), mIL-1β (10ng/ml), mIL-6 (20ng/ml), hTGFβ (2ng/ml)) and T_{reg} (hTGFβ (2ng/ml), hIL-2 (20ng/ml)) polarising conditions for a further 5 days. Supernatants were harvested and cytokine concentrations measured by ELISA (Thermo Fisher).

***Ex vivo* colon organ culture**

3 mm punch biopsies (Miltex) were acquired from murine colons at full thickness. 3 biopsies were cultured in 500 µl of complete animal RPMI for 48 hours in a CO_2 controlled incubator at 37°C and 5% CO_2. Culture supernatants were harvested, and cytokine concentrations measured by ELISA (Thermo Fisher).

ELISA

Cytokine concentrations for IL-17A and IFNγ from the supernatants of cultured cells and ex vivo colon organ cultures were measured by ELISA (Thermo Fisher Ready-Set-Go). Samples and standards were measured in duplicate. Standard curves were created with the standards provided in the kits, in accordance to the manufacturer's protocols.

Flow cytometry

Single cell suspensions extracted from the various tissues were plated out into flow cytometry tubes (Sarstedt) at a concentration of 10^6 cells per ml. Cells were stimulated with 50 ng/ml phorbol 12-myristate 13-acetate (PMA) (Sigma Aldrich) and 1 µg/ml ionomycin (Sigma Aldrich) for 4 hours. For intracellular staining, 2 µM monensin (Sigma Aldrich) was added for the final 2 hours. For intracellular staining, cells were fixed and permeabilised using the Foxp3 fixation/permeabilization buffer kit (BD Biosciences). FcR receptor blocking antibodies were added at a concentration of 1:100 for 15 min at 4°C and surface staining antibodies added together with live/dead stain (Fixable Live/Dead stains Thermo Fisher) and

incubated for 20 mins at room temperature in the dark. Cells were acquired within 24 hours of staining. Fluorochromes were purchased from either BD Biosciences, Biolegend or Thermo Fisher. Fluorochromes used were CD4 (RM4-5), CD8α (53-6.7), CD45.2 (104) CD45.1 (A20), CD3 (17A2), CD5 (53-7.3), CD44 (IM7), CD62L (MEL-14), CD25 (PC61), CD127 (A7R34), CD27 (LG.7F9), CD28 (37.51), CD49d (R1-2), CD95 (15A7), CD11a (M17/4), CD122 (TM-b1), CCR7 (4B12), CXCR3 (CXCR3-173), T-bet (4B10), RORγt (B2D), Foxp3 (FJK-16S), GATA3 (LS0-823), IL-10 (JEs5-16E3), IL-5 (TRFK5), IL-13 (eBio13A), IFNγ (XMG1.2), γδTCR (GL3), CD1d Tetramer (PBS57-loaded or -unloaded, provided by NIH Tetramer Core Facility), B220 (RA3-6B2), DX5 (DX5), CD11c (N418), CD11b (M1/70), Nkp46 (29A1.4), NK1.1 (PK136), c-kit (ACK2), Sca-1 (D7), Haemotopoietic Lineage Cocktail (consisting of: CD3 (17A2), B220 (RA3-6B2), CD11b (M1/70), TER-119 (TER-119), Gr-1 (RB6-8C5)), ICOS (C398.4A). After incubation, cells were washed in sterile PBS and analysed with a LSRFortessa machine (BD Biosciences).

RNA sequencing (RNA-seq)

Naïve and effector memory $CD4^+$ T cells were sorted using the protocol, as described above using anti-CD4-PerCPCy5.5 (RM4-5), anti-CD25-PE (PC61), anti-CD62L-PECy7 (MEL-14; Thermo Fisher) and anti-CD44-Pacific Blue (IM1.8.1; Thermo Fisher). YFP^+ and YFP^- naïve and memory cells were sorted on their basis of YFP expression. Cells were sorted into 1 ml of lysis buffer and either immediately processed for RNA extraction or frozen at -80 for RNA extraction later using the RNAeasy Micro kit (Qiagen). RNA samples were then checked for the quality, contamination and concentration using a NanoDrop, Qubit spectrophotometer and Agilent Bioanalyzer. Libraries were prepared using the Ovation SoLo RNA-seq library preparation kit (NuGEN genomics) according to the manufacturer's protocol and were sequenced on an Illumina HiSeq 3000 to generate 2x75 bp paired-end reads. Reads were filtered to remove adaptors and low-quality bases and aligned to mm9 using TopHat2 [49]. PCR duplicates were removed using the NuGEN duplicate marking tool and read counts generated using featureCounts [50]. Differential gene expression analysis between YFP^+ and YFP^- naïve or YFP^+ and YFP^- T_{EM} $CD4^+$ T cells was conducted using DEseq2 [51], and gene expression levels across all samples were calculated and normalised using the regularized logarithm transformation [51]. GSEA was performed using the fgsea package using 1000 permutations [52] with a T_H1 gene signature identified from comparison between 3 different T_H1 vs T_H2 gene expression datasets [53-55]. Fastq files were downloaded from the SRA and gene centred expression estimates made using kallisto together with the Gencode M20

transcript models. T_H1-specific genes were then identified using DESeq2, with study and cell type (T_H1/T_H2) treated as covariates for batch correction.

Statistical analysis

Statistical analyses were carried using GraphPad Prism 7 (GraphPad Software Inc.). Significance was calculated using the Mann-Whitney test or, for grouped data, the 1-way ANOVA test with Dunn's corrections. P-values <0.05 were judged as significant.

Results

A population of CD4$^+$ T cells with a naïve surface phenotype that have previously expressed T-bet

We generated a fluorescent T-bet fate mapping (T-bet^{FM}) mouse line to identify cells that have expressed T-bet during their ontogeny. We first inserted an IRES-Cre cassette in exon 6 of the endogenous locus *Tbx21* downstream of the stop codon (Supplemental Fig. 1A). These *T-bet$^{cre/+}$* mice were then crossed with *Rosa26$^{YFPfl/+}$* to generate a T-bet^{FM} line in which induction of *Tbx21* triggers *Cre* expression, removal of the *Eyfp* stop codon and thus YFP production (Supplemental Fig. 1B). Thus, this T-bet^{FM} line allows identification of cells that are expressing, or that have previously expressed, T-bet (Supplemental Figs. 1C and D).

We first sought to characterise YFP expression in a basic gating strategy for cell types that are known to express T-bet (Supplemental Figs. 1E-G). We found that 11% of CD4$^+$ T cells and 20% of CD8$^+$ T cells from the spleens of these mice were YFP$^+$. The proportions of F4/80$^+$, CD11c$^+$ and CD19$^+$ cells in the spleen were relatively low (6%, 11% and 3%, respectively; Figs. 1A and B), consistent with the previously characterised expression of T-bet in subsets of these cell types (Refs). In contrast, as expected, 96% of splenic CD45$^+$ NKp46$^+$ lineage$^-$ and CD45$^+$ NKp46$^+$ lineage$^+$ cells were YFP$^+$ (Figs. 1A and B).

We sought to further understand the nature of T-bet expression in CD4$^+$ and CD8$^+$ T cells in spleen and colon. Around a quarter of CD4$^+$ effector memory (T_{EM}) CD4s were YFP$^+$ in both the spleen and the colon (Figs. 1C and D). Some T_{REG} populations have previously been found to express T-bet [21, 56], and, consistent with this, around 6% of splenic and colonic CD4$^+$ CD25$^+$ cells expressed YFP (Figs. 1C and 1D). Only a minority of CD8$^+$ T_{EM} cells were YFP$^+$ whereas, for CD8$^+$ T_{EM} cells, this proportion increased to ~60% in the spleen and 40% in the colon (Figs. 1C and D).

We next turned our attention to naïve (CD62L$^+$ CD44$^-$) CD4$^+$ and CD8$^+$ T cells (Supplemental Figs 1H). T-bet expression is thought to be limited to antigen-experienced T cells. Surprisingly, however, we identified populations of T cells with naïve surface phenotypes that expressed YFP; around 2% of naïve CD4$^+$ cells in the spleen and colon, 16% of naïve CD8$^+$ cells in the spleen and 7% of naïve CD8$^+$ cells in the colon (Figs. 1C and 1D).

To determine whether naïve $CD4^+$ T cells had previously expressed T-bet or were actively expressing T-bet, we utilised a T-bet AmCyan reporter line. We found that around 1% naïve $CD4^+$ T cells and 14% of $CD4^+$ T_{EM} cells were T-bet$^+$ (Figs. 1E and F). We conclude that although T-bet expression is higher in T_{EM} and T_{CM} populations, there exist populations of $CD4^+$ and $CD8^+$ T cells that display evidence of T-bet expression in the context of a seemingly naïve state, which has not previously been reported.

Naïve $CD4^+$ T cells develop and exit the thymus without expressing T-bet

We sought to determine whether the expression of YFP in a proportion of naïve $CD4^+$ T cells indicated prior T-bet expression in the thymus. We found that thymic DN3, DN4, DP and CD4 SP cells completely lacked YFP expression (Figs. 2A and B and Supplemental Fig. 2A). Unexpectedly, DN1 and DN2 populations exhibited a high proportion of YFP-positive cells (32% and 5% respectively; Figs. 2A and B). However, further immunophenotyping demonstrated that the majority (77%) of YFP^+ DN1 cells were in fact NK cells ($CD127^+$ $NK1.1^+$ $CD122^+$; 35% of cells) or NKT cells ($CD122^+$ $NK1.1^+$ $CD3e^+$; 42% of cells; Fig. 2C, Supplemental Fig. 2B). Other YFP-positive cells in the thymus included a small population of effector ($CD62L^-$ $CD44^+$) $CD4^+$ T cells, of which 50% expressed YFP, and 5% of thymic T_{REG} (Figs. 2A and B). However, based on the lack of YFP expression in DN3, DN4, DP and CD4 SP cells, we conclude that mature SP CD4 cells leave the thymus YFP-negative and only express T-bet, becoming YFP-positive, in the periphery.

We next examined YFP expression in γδ T cells (Supplemental Fig. 2C) and NKT cells (Supplemental Fig. 2D), which also arise from the DP stage in the thymus. As expected, no progenitor γδT cells expressed YFP (Figs. 2D and 2E). Surprisingly, however, 20% of immature γδT cells were YFP^+, meaning that some of the cells have expressed T-bet despite not being fully mature (Figs. 2D and 2E). YFP-positivity was primarily associated with IFNγ production, with almost 50% of IFNγ^+ γδ T cells expressing YFP. Interestingly, a small population (8%) of $CD25^-$ IL-17A-producing γδ T cells were also YFP^+ (Figs. 2D and 2E). We conclude that as developing γδ thymocytes mature, there is an increase in the proportion that express YFP, possibly predisposing these cells to becoming T-bet$^+$ IFNγ^+ γδ T cells.

Next, looking at NKT cell development, we found that immature stage 1 cells completely lacked YFP expression and that YFP positivity increased to 5-10% at immature stage 2, 15-

40% at immature stage 3, to finally 60-90% YFP positivity for mature NKT cells (Fig. 2F and 2G).

We conclude from this analysis of the thymus that conventional $CD4^+$ and $CD8^+$ T cells develop in the thymus without expressing YFP and therefore only express T-bet, becoming YFP-positive, once they have left the thymus. However, NKT cells and a subpopulation of γδ T cells, which both require T-bet to develop to maturity, show an increasing proportion of YFP^+ cells in the thymus before leaving the thymus as mature cells.

Naïve $CD4^+$ T cells become YFP^+ shortly after birth

We sought to further characterise the population of YFP^+ naïve-like $CD4^+$ cells using additional cell surface markers and taking cells from different organs within the mice. Dividing cells into naïve ($CD62L^+$ $CD44^-$ $CCR7^+$ $CD28^+$ $CD27^+$), T_{CM} ($CD62L^+$ $CD44^+$ $CCR7^+$ $CD28^+$ $CD27^-$) and T_{EM} ($CD62L^-$ $CD44^+$ $CCR7^-$ $CD28^+$ $CD27^-$) populations revealed that 0.5-1% of definitive naïve $CD4^+$ T cells were YFP^+ (Fig. 3A, 3B). As expected, 15-38% of central memory and 34-74% of $CD4^+$ T_{EM} cells expressed YFP. We conclude that there exists a population of $CD4^+$ T cells with all the hallmarks of the naïve that nevertheless have expressed T-bet.

We next sought to determine whether YFP^+ naïve $CD4^+$ T cells were present before birth, potentially in response to self-antigens, or only arise after birth, potentially due to exposure to environmental antigens. Examination of the fetal liver revealed a lack of YFP^+ naïve or T_{CM} $CD4^+$ cells, but the presence of YFP^+ T_{EM} $CD4^+$ T cells, comprising around 9% of the population (Fig. 3C). We found that by 1-week of age, 1% of naïve $CD4^+$ T cells expressed YFP in the liver, and despite a significant decrease in the liver at 3 weeks of age, the proportion of YFP^+ cells remains consistent afterwards (Fig. 3D and E). A similar pattern was observed in the spleen, with around 0.6% of cells expressing YFP in 1-week old mice, rising significantly to 1.5-2% in older animals (Fig. 3D and E). We conclude that YFP expression, and thus T-bet induction, within naïve T cells occurs shortly after birth. This is consistent with formation of these cells being driven by the microbiota or other environmental factors.

Naïve YFP-positive cells do not correspond to previously defined $CD4^+$ T cell populations

We next sought to determine whether YFP-positive naïve $CD4^+$ T cells might correspond to previously identified naïve-like memory cell populations, in particular memory T cell with naïve-like phenotype (T_{MNP} cells) [41], virtual memory (VM) T cells [37], stem cell-like memory T cells (T_{SCM}) [43, 44], T_H1-like memory phenotype (T_H1-like MP) cells [42] and memory-phenotype (MP) cells [46].

We first measured YFP expression in T_{MNP} cells, which, like naïve cells, are $CD62L^+$ $CD44^-$ $CD28^+$ $CD27^+$, but also $CXCR3^+$ and $CD49d^+$ [41]. In contrast to YFP^+ naïve cells, which were readily detected, we identified very few T_{MNP} cells within the peripheral organs of T-bet^{FM} mice (Supplemental Figure 3A) and none of these cells were YFP^+ (Fig. 4A). In contrast, 0.3% of $CXCR3^-$ $CD49d^-$ naïve CD4 T cells were YFP^+ cells and 16.7% of $CXCR3^+$ $CD49d^-$ cells were also YFP^+ (Fig. 4A). This demonstrated that YFP^+, T-bet-experienced, naïve-like $CD4^+$ T cells do not correspond to T_{MNP} cells. Using the same gating strategy, it was also possible to identify VM cells ($CD62L^-$ $CD44^+$ $CD49^-$ $CXCR3^+$) [57]. 73% of these cells were YFP^+, but since they were not $CD62L^+$ and $CD44^-$, these are distinct from the naïve YFP^+ cell population (Fig. 4A). Finally, using the same gating strategy, we could identify T_H1-like MP cells, which are $CD44^+$ $CD62L^-$ $CXCR3^+$ $CD49d^+$ [42]. Since these T_H1-like MP cells have been shown to express higher levels of T-bet and rapidly produce IFNγ, it was unsurprising to see that 74.2% of these cells were also YFP^+ (Fig. 4A).

We then measured YFP expression in T_{SCM}, which like naïve cells are $CD62L^+$ $CD44^-$ $CD28^+$ $CD27^+$ IL-$7R^+$ but also express the memory cell markers $CD122^+$ and $CD95^+$ [43, 44]. We identified very few of these cells present and found that these were uniformly YFP-negative (Fig. 4B and Supplemental Fig. 3B). In contrast, 0.6% of the canonical naïve $CD4^+$ population ($CD62L^+$ $CD44^-$ $CD28^+$ $CD27^+$ IL-$7R^+$ $CD122^-$ $CD95^-$) were YFP^+ (Fig. 4B). Thus, naïve YFP^+ $CD4^+$ T cells are distinct from T_{SCM}.

We next examined YFP expression in MP cells, which have been found to differentiate from a population of $CD5^{hi}$ naïve cells in the absence of foreign antigen and exist in T-bet^{lo}, T-bet^{int} and T-bet^{hi} states [46]. We found that only a minority of naïve $CD5^+$ cells were YFP^+; around 2% in the spleen, 6% in the mLN, 4% in the colon and 1% in the liver (Fig. 4C). Thus, we have shown here that these naïve YFP^+ cells and MP cells are both $CD5^{hi}$.

Lastly, we sought to investigate potential differences in the expression of the typical activated memory markers CD122, CD49d and CXCR3 on between YFP^+ and YFP^+ $CD4^+$ naïve ($CD62L^+$ $CD44^-$) and T_{EM} ($CD62L^-$ $CD44^+$) cells. We found that both YFP^- and YFP^+ naïve $CD4^+$ T cells exhibited lower levels of CD49d and CD122 in comparison to both YFP^+ and YFP^- T_{EM} populations (Fig. 4D). This again suggests that YFP^+ naive cells are not a memory population. Interestingly, when comparing YFP^+ naïve against YFP^- naïve T cells, the only major difference in surface marker expression was CXCR3, which was present on 30% of YFP^+ naïve cells compared with only 3% of YFP^- naïve $CD4^+$ T cells (Fig. 4E). We conclude that YFP^+ naïve $CD4^+$ T cells share naïve surface markers with YFP^- naïve $CD4^+$ T cells except for an increased CXCR3 expression and do not represent a previously described T cell subset. Given this characterisation, we will refer to the phenotype of these cells as naïve from here on in.

YFP^+ naïve $CD4^+$ T cells are predisposed to produce IFNγ upon activation

We hypothesised that YFP^+ naïve cells may possess distinct properties to YFP^- naïve cells and that their experience of T-bet expression may allow rapid upregulation of IFNγ. To test this, we purified YFP^- and YFP^+ naïve ($CD62L^+$ $CD44^-$) and T_{EM} ($CD62L^-$ $CD44^+$) $CD4^+$ T cells, activated these cells *in vitro* in non-polarising conditions and measured cytokine production and T-bet expression by ELISA and flow cytometry. Stimulation of naive YFP^+ cells in non-polarising conditions caused robust induction of IFNγ production that was not observed in the YFP^- population (Fig. 5A, Supp Fig. 4A). In contrast, there was no production of IL-17A, demonstrating that naïve YFP^+ cells are specifically polarised towards the T_H1 lineage. T-bet was present in over 90% of IFNγ-producing YFP^+ naïve cells, whereas YFP^- naïve cells lacked T-bet expression (Fig. 5A). We also examined the effect of stimulation on cytokine production by YFP^+ T_{EM} cells. As we found for their naïve counterparts, YFP^+ T_{EM} cells expressed IFNγ, but not IL-17A, whereas YFP^- effector cells expressed either IFNγ or IL-17A (Fig. 5B, Supp Fig. 4A).

We next sought to determine whether the predisposition of YFP^+ naïve cells to produce IFNγ was stable under T_H2, T_H17 and iT_{reg} polarising conditions. The naïve YFP^+ population resisted induction of IL-4 or IL-17A after culture in T_H2 or T_H17 -polarising conditions, respectively (Figs. 5C and 5D). Similarly, compared to YFP^- naïve cells, a greater proportion of YFP^+ naïve cells maintained IFNγ production under T_H2 and iT_{REG}-polarising conditions, although induction was weakened compare to T_H1 conditions (Fig. 5C and 5D). We conclude

that naïve YFP^+ cells are predisposed to produce IFNγ over cytokines of other T cell lineages when polarised *in vitro*.

Naïve and T_{EM} YFP^+ $CD4^+$ T cells are polarised towards a T_H1 phenotype

We wished to determine whether the predisposition of YFP^+ naïve cells to produce IFNγ reflected polarisation towards the T_H1 lineage. To test this, we compared the gene expression profiles of YFP^+ versus YFP^- naïve and $CD62L^-$ $CD44^+$ T_{EM} $CD4^+$ T cells using RNA-seq. Visualising the relationship between the expression profiles of the four cell populations, we found that YFP^+ naïve and YFP^+ T_{EM} cells were distinct from their YFP^- counterparts, with YFP^+ naïve cells being more similar to YFP^- naïve cells than to either of the T_{EM} cell populations (Fig. 5E and Supplemental Fig. 4B). This is consistent with our flow cytometric analyses showing that YFP^+ naïve cells display the hallmarks of a naïve cell population.

We next sought to identify the genes that distinguished YFP^+ naïve cells from YFP^- naïve cells. We found that YFP^+ cells exhibited high levels of expression of a number of T-bet target genes that mark T_H1 cells, including *Tbx21, Ifng, Cxcr3, Ccl4, Ccl5, Itgb1, Havcr2, Nkg7, Il12rb1* and *Il18rap*, and genes encoding transcription factors that cooperate with T-bet, including *Zeb2, Hopx* and *Bhlhe40* (Fig. 5F). Consistent with this, gene set enrichment analysis (GSEA) confirmed enrichment of T_H1 genes within the set of genes highly expressed in YFP^+ versus YFP^- naïve cells (Supp. Fig. 4C). Thus, these data demonstrate that YFP^+ naïve cells are polarised towards a T_H1 lineage phenotype. We also noted higher expression of *Foxp3*, *Ikzf2* (Helios) and *Nrp1*, required for T_{REG} function, suggesting there might also be heterogeneity within the YFP^+ naïve cell population.

We next turned our attention to the expression profile of YFP^+ T_{EM} cells compared to their YFP^- counterparts. As for the naïve cells, we identified higher expression of a number of T_H1 genes, including *Ifng, Tbx21, Cxcr3, Ccl5, Il12rb2, Il18rap, Nkg7, Prf1 and Fasl* (Fig. 5G). YFP^+ T_{EM} cells also exhibited reduced expression of a broad set of genes suggesting that in this differentiated population, the repression of alternative differentiation pathways is a key function of T-bet expression. We conclude that YFP^+ naïve and memory subsets have distinct gene expression profiles from their YFP^- counterparts, which is consistent with T-bet function in these cells.

Naïve YFP^+ $CD4^+$ T cells remain T_H1 polarised in a murine T_H1/T_H17 model of colitis

The role of T_H1 and T_H17 cells in inflammatory disease is reflected by the induction of colitis upon adoptive transfer of naïve $CD4^+$ T cells into *Rag2*$^{-/-}$ mice, which is marked by a wasting phenotype, inflamed colons, splenomegaly and a T_H1, T_H17 and T_H1/T_H17 dual/hybrid-driven inflammatory response [25]. To test whether the T_H1 polarised phenotype of YFP^+ naïve cells altered their ability to induce inflammatory disease, we transferred either 25,000 YFP^- or YFP^+ naïve $CD4^+$ T cells into separate *Rag2*$^{-/-}$ mice and observed disease symptoms and cytokine production in colon organ cultures and in unfractionated cells from spleen, mLN and colon by ELISA. Neither group of mice developed wasting disease, most likely due to the small number of naïve T cells available for transfer, however both sets of recipient mice gained less weight compared to control mice (Fig. 6A). Next, examining colon and spleen weights, we found that mice receiving YFP^+ naïve T cells had smaller colons ($p<0.05$) and spleens in comparison with YFP^- naïve T cell recipient mice (Fig. 6B), suggesting that YFP^+ $CD4^+$ T cells induced less inflammation than their YFP^- counterparts. Donor $CD4^+$ T cells could be detected in the colon, mLN and spleen after 9 weeks of transfer. Measuring cytokine production by donor cells in these organs, we found no difference in the proportion of IFNγ-producing $CD4^+$ T cells in YFP^+ versus YFP^- treated mice (Figs. 6C and D). There was a slight decrease in IL-17A producers in the colon from YFP^+ transferred mice, although this was not significant. However, the level of IFNγ production measured by ELISA in the supernatant from colonic biopsy organ culture (Supplemental Fig. 5A) and from bulk cultured cells (Supplemental Fig. 5B) from the colon from YFP^+ naïve T cell recipient mice was significantly greater than for YFP^- naïve T cell recipients. This demonstrates that either the predisposition of YFP^+ $CD4^+$ T cells to produce IFNγ is maintained *in vivo* or that receipt of YFP^+ $CD4^+$ T cells increases IFNγ production by other cells in the mice.

In order to test whether YFP^+ naïve $CD4^+$ T cells were fixed to producing IFNγ even in the T_H17-polarising environment of the T cell transfer colitis model, we co-transferred a total of 50,000 naïve CD45.2 YFP^+ $CD4^+$ T cells and naïve CD45.1 $CD4^+$ T cells at a ratio of 10:90 (CD45.2 YFP^+: CD45.1) into *Rag2*$^{-/-}$ mice. Co-transfer of both cell populations produced a wasting phenotype indicative of disease in this colitis model (Supplemental Fig. 5C). The transferred YFP^+ CD45.2 population contained significantly more IFNγ-positive cells and lacked IL-17A-positive cells, as expected, compared to CD45.1 cells, which were able to produce IL-17A (Figs. 6E and 6F). We conclude that YFP^+ naïve $CD4^+$ T cells remain polarised to the T_H1 lineage, even in a T_H1/T_H17-driven colitis model *in vivo*.

Discussion

Here, we report the use of a novel T-bet^{FM} mouse line to identify cells that have expressed the T_H1 lineage-specifying transcription factor T-bet. The T-bet^{FM} mouse line has allowed confirmation of known T-bet expressing lineages and revealed previously uncharacterised T-bet expressing cell populations. We identify a distinct sub-population of CD4+ T cells that have a naïve surface phenotype but that have experienced T-bet expression. The cells arise after birth, exhibit a T_H1 expression profile and rapidly upregulate IFNγ upon activation. The T_H1 phenotype is stable both in repolarising conditions in vitro and in a T_H1/T_H17-driven inflammatory disease model in vivo. We conclude that T-bet expression defines a population of T_H1-polarised naïve-like cells that function to shape subsequent T helper cell responses.

The pattern of YFP positivity, marking cells that have experienced T-bet expression, recapitulates previous knowledge of T-bet function. For example, the expression of T-bet in developing NKT cells and γδ T cells in the thymus [58-61]. Interestingly, as described previously, IFNγ-producing γδ T cells express T-bet and IL-17A producing γδ T cells express RORγt. However, our data suggests that a subset of IL-17A producing γδ T cells has also expressed T-bet. Further phenotyping of these γδ T cells would be required to identify the different Vγ variable regions within these subsets [62]. As expected, developing thymic SP $CD4^+$ and $CD8^+$ T cells and DP cells were all YFP negative. All cell types in the periphery that were expected to express T-bet - NK cells, $CD4^+$ T_{EM} and T_{CM} and $CD8^+$ T_{EM} and T_{CM} - were positive for YFP [2, 61, 63-69].

Unexpectedly, we found that populations of $CD4^+$ T cells with naïve markers in the peripheral blood were YFP^+. We could also detect ongoing T-bet expression in a subset of naïve $CD4^+$ T cells in T-bet^{Amcyan} reporter mice. Characterisation of YFP^+ naïve $CD4^+$ T cells revealed them to lack the markers of T_{SCM}, T_{MNP}, T_H1-like MP or VM cells [41-43, 57, 70, 71] and thus represent a novel cell population. YFP^+ naïve CD4 cells were $CD5^{high}$ and since MP cells have been shown to also be $CD5^{high}$, we suggest that these could the same cells. These YFP^+ naïve cells may be related to precursors to the T-bet^{hi} MP cells but might not be the MP cells themselves. However, further phenotyping and functional responses to *T.gondii* and other external pathogens would be needed in order to confirm this [46]. Interestingly,

30% of the YFP^+ naïve CD4 T cells were positive for CXCR3. CXCR3, a known T-bet target gene, is required for the migration of both $CD4^+$ and $CD8^+$ T cells to sites of inflammation [5, 72-74]. Thus, YFP^+ $CXCR3^+$ $CD4^+$ T cells could be predetermined early immune responders that are able to migrate to areas of infection where they can rapidly induce a T_H1 response.

We found that YFP^+ cells are absent from foetuses and only develop after birth, when they become visible from as early as 1 week of age and remain throughout the lifespan of the mice. This suggests a requirement for an environmental antigen. This further supports the idea that YFP^+ naïve $CD4^+$ T cells are predisposed early inflammatory responders that react to environmental antigens.

In vitro and *in vivo* analyses of YFP^+ naïve T cells show that they have a different phenotype to their YFP^- counterparts. The cells exhibit a T_H1 expression profile and produce high amounts of IFNγ upon activation. YFP^+ naïve T cells also resist polarisation to different lineages both *in vitro* and in a T_H1/T_H17-driven colitis model *in vivo*. These data are again consistent with a role for these cells as early T_H1-polarised responders whose role is to produce IFNγ within inflammatory environments. These data also suggested that the YFP^+ naïve T cells are unable to initiate an colitogenic phenotype on their own due to their lack of IL-17A production, which is required for induction of colitis in the naïve T cell transfer model [15, 23-27]. These data further emphasised that YFP^+ naïve CD4 T cells are fixed to rapidly produce IFNγ.

The expression of a T-bet in cells that are otherwise naïve suggests that lineage specification can proceed in the absence of overt T cell activation. Identification of signals responsible for T-bet upregulation, and why these have such subtle effects on the phenotypes of the cells, will require further investigation. The use of fate mapper mouse models to study the expression or activation of other T cell lineage-specifying factors will also reveal whether this is a more general phenomenon.

In conclusion, we have identified a $CD4^+$ T cell subset with a naïve surface phenotype that has experienced T-bet expression, is pre-polarised to the T_H1 lineage, and which provides a rapid and stable source of IFNγ upon activation. This has implications for our understanding of the mechanisms that shape T helper responses in infection and inflammatory disease.

Acknowledgements

This study was supported by grants awarded by the Medical Research Council (RGJ and GML grant numbers MR/M003493/1 and MR/R001413/1) and a CRUK PhD studentship supporting MVdM awarded to RGJ. Research was also supported by the BRC Flow Core facility at Guy's and St Thomas' NHS Foundation Trust and UCL. RNA-seq was performed by Paola Niola at UCL Genomics.

Author Contributions

Study concept and design (JWL, GML, RGJ), data acquisition (JWL, MVdM, LR), data analysis and interpretation (JWL, MVdM, SH, LR), technical support (LR, NG, AH, JFN, ES, IJ), obtaining funding (RGJ, GML, JKH), writing the manuscript (JWL, RGJ, MVdM), study supervision (RGJ, GML).

Data Availability

RNA-seq data have been deposited in the Gene Expression Omnibus (GEO) with accession code GSE153805. This can be accessed with the secure token enufyogsxrutzut.

Figure Legends

Figure 1. T-bet fate mapping identifies a population of peripheral naïve-like CD4$^+$ T cells that have experienced T-bet expression.

A. Representative flow plots showing YFP expression in different splenic cells populations.

B. Quantification of the proportions of YFP$^+$ cells for each cell type shown in A (n=3).

C. Representative flow plots showing YFP expression in naïve CD4$^+$ T cells (CD3$^+$ CD4$^+$ CD8$^-$ CD25$^-$ CD62L$^+$ CD44$^-$), effector CD4$^+$ T cells (CD3$^+$ CD4$^+$ CD8$^-$ CD25$^-$ CD62L$^-$ CD44$^+$), regulatory T cells (CD3$^+$ CD4$^+$ CD8$^-$ CD25$^+$), naïve CD8$^+$ T cells (CD3$^+$ CD4$^-$ CD8$^+$ CD62L$^+$ CD44$^-$), effector CD8$^+$ T cells (CD3$^+$ CD4$^-$ CD8$^+$ CD62L$^-$ CD44$^+$) and central memory CD8$^+$ T cells (CD3$^+$ CD4$^-$ CD8$^+$ CD62L$^+$ CD44$^+$) from the spleen (above) and colon (below).

D. Mean proportions of YFP$^+$ cells from the different subtypes of T cells in the spleen (n=9) and colon shown in in E (n=6).

E. Representative flow plot showing the proportion of CD3$^+$ CD4$^+$ naïve or T_{EM} cells expressing AmCyan in the T-bet^{AmCyan} mouse reporter line.

F. Overall dot plot showing the proportion of CD3$^+$ CD4$^+$ naïve or T_{EM} cells expressing AmCyan in the T-bet^{AmCyan} mouse reporter line (n=4).

Figure 2. Naïve $CD4^+$ T cells develop and exit the thymus without expressing T-bet.

A. Representative flow plots showing YFP expression in thymic DN1 ($CD3^-$ $CD44^+$ $CD25^-$), DN2 ($CD3^-$ $CD44^+$ $CD25^+$), DN3 ($CD3^+$ $CD44^-$ $CD25^+$), DN4 ($CD3^+$ $CD44^-$ $CD25^-$), DP ($CD3^+$ $CD4^+$ $CD25^+$), naïve $CD4^+$ T cells ($CD3^+$ $CD4^+$ $CD8^-$ $CD62L^+$ $CD44^-$), memory $CD4^+$ T cells ($CD3^+$ $CD4^+$ $CD8^-$ $CD62L^-$ $CD44^+$) and regulatory $CD4^+$ T cells ($CD3^+$ $CD4^+$ $CD8^-$ $CD25^+$).

B. Mean proportions of YFP^+ cells in the different thymic cell subsets shown in A (n=12).

C. Representative flow plots of NK and NKT markers on YFP^+ cells from DN1 (live $CD4^-$ $CD8^-$ $CD44^+$ $CD25^-$ $CD122^+$ $NK1.1^+$) and DN2 (live $CD4^-$ $CD8^-$ $CD44^+$ $CD25^+$ $CD122^+$ $NK1.1^+$) cells from the thymus.

D. Representative flow plots showing YFP expression in five populations of developing γδT cells in the thymus: progenitor γδT cells ($CD25^+$ $CD27^+$ $CD24^+$), immature γδT cells ($CD25^-$ $CD27^+$ $CD24^+$), IFNγ-producing γδT cells ($CD25^-$ $CD24^-$ $CD27^+$) and the two IL-17A-producing γδT cells ($CD25^-$ $CD27^-$ $CD24^-$ and $CD25^+$ $CD27^-$ $CD24^+$).

E. Mean proportions of YFP^+ cells from the different stages of γδT cells development shown in D (n=6).

F. Representative flow plots showing YFP expression in the four populations of developing NKT cells in the thymus: Immature 1 ($CD44^-$ $CD24^+$), immature 2 ($CD44^-$ $CD24^-$), immature 3 ($CD44^+$ $CD24^-$ $NK1.1^-$) and mature NKT cells ($CD44^+$ $NK1.1^+$).

G. Mean proportions of YFP^+ cells from the different stages of NKT cell development shown in F (n=12).

Figure 3. Naïve $CD4^+$ T cells become YFP^+ shortly after birth.

A. Representative flow plots showing YFP expression in the naïve $CD4^+$ T cells (live $CD3^+$ $CD4^+$ $CD62L^+$ $CD44^-$ $CCR7^+$ $CD28^+$ $CD27^+$), effector $CD4^+$ T cells (live $CD3^+$ $CD4^+$ $CD62L^-$ $CD44^+$ $CCR7^-$ $CD28^+$ $CD27^-$) and central memory $CD4^+$ T cells (live $CD3^+$ $CD4^+$ $CD62L^-$ $CD44^+$ $CCR7^-$ $CD28^-$ $CD27^-$) in the thymus, spleen, colon, mesenteric lymph nodes, peripheral lymph nodes and liver.

B. Mean proportions of YFP^+ cells in naïve, effector memory and central memory $CD4^+$ T cell populations shown in A (n=3 for thymus, colon, pLN, n=5 for liver, n=6 for mLN and n=8 for spleen).

C. Representative flow plots showing YFP expression in naïve ($CD62L^+$ $CD44^-$), effector ($CD62L^-$ $CD44^+$) and central memory ($CD62L^+$ $CD44^+$) $CD4^+$ T cells in the foetal liver, adult liver and adult spleen.

D. Representative flow plots showing YFP expression in splenic naïve ($CD62L^+$ $CD44^-$) $CD4^+$ T cells from 1-week (n=5), 3-week (n=6), 8-week (n=8), 25-week (n=4) and 50-week (n=4) old mice.

E. Mean proportions of YFP^+ cells in naïve ($CD62L^+$ $CD44^-$) $CD4^+$ T cells from 1-week (n=5), 3-week (n=6), 8-week (n=8), 25-week (n=4) and 50-week (n=4) old mice. * = $P<0.05$, ** = $P<0.01$ (Kruskal-Wallis test performed with Dunn's corrections)

Figure 4. YFP-positive naïve-like cells do not correspond to previously defined CD4 T cell populations

A. Representative flow plots showing YFP expression in splenic $CD28^+$ $CD27^+$ T cell populations divided by CD62L, CD44, CXCR3 and CD49d expression. Naïve ($CD62L^+$ $CD44^-$ $CXCR3^-$ $CD49d^-$), T_{MNP} ($CD62L^+$ $CD44^-$ $CXCR3^+$ $CD49d^+$), T_H1-like MP ($CD62L^-$ $CD44^+$ $CD49d^+$ $CXCR3^+$) and VM ($CD62L^-$ $CD44^+$ $CD49d^-$ $CXCR3^+$) T cell populations are labelled.

B. Representative flow plots showing YFP expression by conventional naïve $CD4^+$ T cells ($CD62L^+$ $CD44^-$ $CD28^+$ $CD27^+$ $CD127^+$ $CD122^-$ $CD95^-$) compared with T_{SCM} ($CD62L^+$ $CD44^-$ $CD28^+$ $CD27^+$ $CD127^+$ $CD122^+$ $CD95^+$) from the spleen.

C. Representative flow plots and mean proportions of naïve YFP^+ $CD5^+$ $CD4^+$ T cells (live $CD3^+$ $CD4^+$ $CD62L^+$ $CD44^-$) in the spleen, mLN and colon (n=6 for spleen and mLN, n=5 for colon and n=4 for liver).

D. Representative histograms showing surface marker expression in YFP^- vs YFP^+ naïve (live $CD3^+$ $CD4^+$ $CD62L^+$ $CD44^-$) and effector memory (live $CD3^+$ $CD4^+$ $CD62L^-$ $CD44^+$) $CD4^+$ T cells from the spleen.

Figure 5. YFP$^+$ naïve-like CD4$^+$ T cells are polarised towards the T_H1 lineage.

A. Representative flow plots showing cytokine expression (top) or T-bet and YFP expression (bottom) in YFP$^-$ and YFP$^+$ naive (CD62L$^+$CD44$^-$) CD4$^+$ T cells after activation with anti-CD3/CD28 and culture with IL-2.

B. Representative flow plots showing cytokine expression from *in vitro* cultured YFP$^-$ and YFP$^+$ memory (CD62L$^-$CD44$^+$) CD4$^+$ T cells after activation with anti-CD3/CD28 and culture with IL-2.

C. Representative flow plots showing cytokine expression in naïve (CD62L$^+$ CD44$^-$) CD4$^+$ T cells after activation with anti-CD3/CD28 activation and polarisation in T_H1, T_H2 T_H17 and iT_{REG} conditions *in vitro* (n=6).

D. Cytokine expression (mean and SEM (n=6)) in naïve (CD62L$^+$ CD44$^-$) CD4$^+$ T cells after activation with anti-CD3/CD28 and polarisation in T_H1, T_H2 T_H17 and iT_{REG} conditions *in vitro*.

E. PCA plot showing the relationship between the gene expression profiles of YFP$^+$ and YFP$^-$ naïve (live CD3$^+$ CD4$^+$ CD62L$^+$ CD44$^-$) and T_{EM} (live CD3$^+$ CD4$^+$ CD62L$^-$ CD44$^+$) CD4$^+$ T cell populations.

F. Volcano plot showing differential gene expression between YFP$^+$ and YFP$^-$ naïve CD4$^+$ T cells (log2 fold change vs adjusted p-value). Genes more highly expressed in YFP$^+$ cells are in red and those more highly expressed in YFP$^-$ cells are in blue. Selected differentially expressed genes are labelled.

G. Volcano plot showing differential gene expression between YFP$^+$ and YFP$^-$ T_{EM} CD4$^+$ T cells (log2 fold change vs adjusted p-value). Genes more highly expressed in YFP$^+$ cells are in red and those more highly expressed in YFP$^-$ cells are in blue (p_{adj} <0.05, |log2FC|>1). Selected differentially expressed genes are labelled.

Figure 6. YFP$^+$ cells induce less inflammation but more IFNγ compared to conventional naïve CD4$^+$ T cells after transfer to *Rag2*$^{-/-}$ mice.

A. Weight change in *Rag2*$^{-/-}$ mice after receipt of no T cells or 25,000 purified naïve YFP$^+$ or naïve YFP$^-$ CD4$^+$ T cells (n=3 for each transfer and n=7 for control).

B. Spleen and colon mass in *Rag2*$^{-/-}$ mice after receipt of no T cells or 25,000 purified naïve YFP$^+$ or naïve YFP$^-$ CD4$^+$ T cells (n=3 for each transfer and n=7 for control) * $P<0.05$.

C. Representative flow plots showing the proportion of YFP$^-$ and YFP$^+$ naïve CD4$^+$ T cells that produce IFNγ and IL-17A after transfer into *Rag2*$^{-/-}$ mice, separated by organ.

D. Mean proportion of YFP$^-$ and YFP$^+$ naïve CD4$^+$ T cells shown in C that produce IFNγ and IL-17A after transfer into *Rag2*$^{-/-}$ mice, separated by organ (n=3 for each transfer).

E. Mouse weights after co-transfer of 50,000 naïve (CD62L$^+$ CD44$^-$) CD45.1 and CD45.2 YFP$^+$ CD4$^+$ T cells at a ratio of 90:10 in *Rag2*$^{-/-}$ mice (n=5).

F. Representative flow plots showing IFNγ and IL-17A production by naïve CD45.1$^+$ and CD45.2 YFP$^+$ CD4$^+$ T cells after co-transfer 90:10.

G. Mean proportions of naïve CD45.1 and CD45.2 YFP$^+$ CD4$^+$ T cells producing IFNγ after co-transfer into *Rag2*$^{-/-}$ mice at a ratio of 90:10 (n=5). *** $P<0.001$ when using non-parametric multiple t-test.

Supplemental Figure Legends

Supplemental Figure 1. Characterising YFP expression in the T-bet^{FM} mouse.

A. Schematic showing the insertion of *Cre* into exon 6 of *Tbx21*.

B. Schematic showing the generation of the T-bet^{cre} x ROSA26YFP$^{fl/fl}$ mouse line.

C. Representative flow plots showing cytokine and YFP expression in naïve (CD62L^{+} CD44^{-}) CD4^{+} T cells after activation with anti-CD3/CD28 activation and polarisation in T_H1 and T_H2 conditions.

D. Representative histogram showing T-bet expression of IFNγ^{+} YFP^{+} and IFNγ^{-} YFP^{-} cells.

E. Representative flow plots showing the gating strategy for NK-like and NKT-like cells.

F. Representative flow plots showing the gating strategy for lymphoid cells.

G. Representative flow plots showing the gating strategy for myeloid cells.

H. Representative flow plots showing the gating for CD4^{+} and CD8^{+} T cell subsets in the spleen and colon.

Supplemental Figure 2. YFP expression in cells of the thymus.

A. Representative flow plots showing the gating strategy used for cells in the thymus.

B. Representative flow plots showing the proportion of YFP^- and YFP^+ DN1 cells expressing NK and NKT markers.

C. Representative flow plots showing the gating strategy used to identify γδT cells in the thymus.

D. Representative flow plots showing the gating strategy used to identify NKT cell in the thymus.

Supplemental Figure 3. Gating strategies for T_{SCM}, VM, T_H1-like MP and T_{MNP} $CD4^+$ T cells.

A. Gating strategy shown for identifying T_{MNP}, T_H1-like MP and VM T cells in the naïve ($CD62L^+$ $CD44^-$) compartment in the spleen.

B. Gating strategy shown for identifying T_{SCM} in the naïve ($CD62L^+$ $CD44^-$) compartment in the spleen.

Supplemental Figure 4. YFP$^+$ naïve-like CD4$^+$ T cells are predisposed to produce IFNγ upon activation.

A. IFNγ and IL-17A in the supernatant of the cultured cells measured by ELISAs (n=6, except n=2 for YFP$^+$ naïve CD4 T cells). * = P<0.05 (Kruskal-Wallis test performed with Dunn's corrections)

B. Representative flow plots showing YFP and IFNγ expression by naïve (CD62L$^+$ CD44$^-$) YFP$^-$ and YFP$^+$ CD4$^+$ T cells after activation with anti-CD3/CD28 and culture with IL-2 for 3, 5 and 7 days.

C. Mean proportions of naïve (CD62L$^+$ CD44$^-$) CD4$^+$ T cells shown in B that produce IFNγ after 3, 5 and 7 days of culture (n=3 for day 5 and 7 and n=1 for day 3).

D. Heatmap from RNA-sequencing showing the fold change in gene expression between sorted naïve (CD62L$^+$ CD44$^-$) CD4$^+$ YFP$^-$, naïve CD4$^+$ YFP$^+$, effector memory (CD62L$^-$ CD44$^+$) CD4$^+$ YFP$^-$ and effector memory CD4$^+$ YFP$^+$ (n=3).

E. Gene set enrichment analysis (GSEA) confirming enrichment of T_H1 genes within the naïve YFP$^+$ CD4$^+$ cells versus naïve YFP$^-$ CD4$^+$ cells.

Supplemental Figure 5. Naive YFP$^+$ cells maintain stable IFNγ production and lack IL-17A production in a T cell transfer-induced colitis model.

A. Quantification of IFNγ and IL-17A in the supernatant by ELISA after 48 hours of colon organ culture (n= 3, except n=6 for the no transfer control). * $P<0.05$

B. Quantification of IFNγ and IL-17A in the supernatant of unfractionated cell cultures from colon, spleen and mLN (n= 3, except n=6 for the no transfer control). * $P<0.05$

References

1. Mosmann, T.R., et al., *Two types of murine helper T cell clone. I. Definition according to profiles of lymphokine activities and secreted proteins.* The Journal of Immunology, 1986. **136**(7): p. 2348.
2. Szabo, S.J., et al., *A novel transcription factor, T-bet, directs Th1 lineage commitment.* Cell, 2000. **100**(6): p. 655-69.
3. Lazarevic, V., L.H. Glimcher, and G.M. Lord, *T-bet: a bridge between innate and adaptive immunity.* Nature Reviews Immunology, 2013. **13**: p. 777.
4. Jenner, R.G., et al., *The transcription factors T-bet and GATA-3 control alternative pathways of T-cell differentiation through a shared set of target genes.* Proceedings of the National Academy of Sciences, 2009. **106**(42): p. 17876.
5. Lord, G.M., et al., *T-bet is required for optimal proinflammatory CD4⁺ T-cell trafficking.* Blood, 2005. **106**(10): p. 3432.
6. Mullen, A.C., et al., *Role of T-bet in commitment of TH1 cells before IL-12-dependent selection.* Science, 2001. **292**(5523): p. 1907-10.
7. Szabo, S.J., et al., *Molecular Mechanisms RegulatinG Th1 Immune Responses.* Annual Review of Immunology, 2003. **21**(1): p. 713-758.
8. Kanhere, A., et al., *T-bet and GATA3 orchestrate Th1 and Th2 differentiation through lineage-specific targeting of distal regulatory elements.* Nature Communications, 2012. **3**: p. 1268.
9. Avni, O., et al., *T(H) cell differentiation is accompanied by dynamic changes in histone acetylation of cytokine genes.* Nat Immunol, 2002. **3**(7): p. 643-51.
10. Fields, P.E., S.T. Kim, and R.A. Flavell, *Cutting edge: changes in histone acetylation at the IL-4 and IFN-gamma loci accompany Th1/Th2 differentiation.* J Immunol, 2002. **169**(2): p. 647-50.
11. Messi, M., et al., *Memory and flexibility of cytokine gene expression as separable properties of human T(H)1 and T(H)2 lymphocytes.* Nat Immunol, 2003. **4**(1): p. 78-86.
12. Usui , T., et al., *T-bet regulates Th1 responses through essential effects on GATA-3 function rather than on IFNG gene acetylation and transcription.* Journal of Experimental Medicine, 2006. **203**(3): p. 755-766.
13. Hwang, E.S., et al., *T Helper Cell Fate Specified by Kinase-Mediated Interaction of T-bet with GATA-3.* Science, 2005. **307**(5708): p. 430.
14. Lazarevic, V., et al., *T-bet represses T(H)17 differentiation by preventing Runx1-mediated activation of the gene encoding RORgammat.* Nat Immunol, 2011. **12**(1): p. 96-104.
15. Gökmen, M.R., et al., *Genome-wide regulatory analysis reveals T-bet controls Th17 lineage differentiation through direct suppression of IRF4.* Journal of immunology (Baltimore, Md. : 1950), 2013. **191**(12): p. 10.4049/jimmunol.1202254.
16. O'Shea, J.J., et al., *Genomic views of STAT function in CD4+ T helper cell differentiation.* Nature Reviews Immunology, 2011. **11**: p. 239.
17. Evans, C.M. and R.G. Jenner, *Transcription factor interplay in T helper cell differentiation.* Briefings in functional genomics, 2013. **12**(6): p. 499-511.
18. Ghoreschi, K., et al., *Generation of pathogenic TH17 cells in the absence of TGF-β signalling.* Nature, 2010. **467**(7318): p. 967-971.
19. Lee, Y., et al., *Induction and molecular signature of pathogenic TH17 cells.* Nature Immunology, 2012. **13**(10): p. 991-999.

20. Yang, Y., et al., *T-bet is essential for encephalitogenicity of both Th1 and Th17 cells.* Journal of Experimental Medicine, 2009. **206**(7): p. 1549-1564.
21. Koch, M.A., et al., *T-bet controls regulatory T cell homeostasis and function during type-1 inflammation.* Nature Immunology, 2009. **10**(6): p. 595-602.
22. Monteleone, I., et al., *Regulation of the T helper cell type 1 transcription factor T-bet in coeliac disease mucosa.* Gut, 2004. **53**(8): p. 1090-5.
23. Neurath, M.F., et al., *The transcription factor T-bet regulates mucosal T cell activation in experimental colitis and Crohn's disease.* The Journal of experimental medicine, 2002. **195**(9): p. 1129-1143.
24. Krausgruber, T., et al., *T-bet is a key modulator of IL-23-driven pathogenic CD4+ T cell responses in the intestine.* Nature Communications, 2016. **7**(1): p. 11627.
25. Powrie, F., et al., *Phenotypically distinct subsets of CD4+ T cells induce or protect from chronic intestinal inflammation in C. B-17 scid mice.* International Immunology, 1993. **5**(11): p. 1461-1471.
26. Powrie, F., S. Mauze, and R.L. Coffman, *CD4+ T-cells in the regulation of inflammatory responses in the intestine.* Research in Immunology, 1997. **148**(8): p. 576-581.
27. Ostanin, D.V., et al., *T cell transfer model of chronic colitis: concepts, considerations, and tricks of the trade.* American Journal of Physiology - Gastrointestinal and Liver Physiology, 2009. **296**(2): p. G135-G146.
28. Ariga, H., et al., *Instruction of naive CD4+ T-cell fate to T-bet expression and T helper 1 development: roles of T-cell receptor-mediated signals.* Immunology, 2007. **122**(2): p. 210-221.
29. Placek, K., et al., *Integration of Distinct Intracellular Signaling Pathways at Distal Regulatory Elements Directs T-bet Expression in Human CD4⁺ T Cells.* The Journal of Immunology, 2009. **183**(12): p. 7743.
30. Hu, J. and A. August, *Naïve and Innate Memory phenotype CD4(+) T-cells have different requirements for active Itk for their development.* Journal of immunology (Baltimore, Md. : 1950), 2008. **180**(10): p. 6544-6552.
31. Sallusto, F., et al., *Two subsets of memory T lymphocytes with distinct homing potentials and effector functions.* Nature, 1999. **401**: p. 708.
32. Zhu, J., H. Yamane, and W.E. Paul, *Differentiation of Effector CD4 T Cell Populations.* Annual review of immunology, 2010. **28**: p. 445-489.
33. Berard, M. and D.F. Tough, *Qualitative differences between naïve and memory T cells.* Immunology, 2002. **106**(2): p. 127-138.
34. Weinreich, M.A., et al., *T cells expressing the transcription factor PLZF regulate the development of memory-like CD8+ T cells.* Nat Immunol, 2010. **11**(8): p. 709-16.
35. Cheroutre, H., F. Lambolez, and D. Mucida, *The light and dark sides of intestinal intraepithelial lymphocytes.* Nat Rev Immunol, 2011. **11**(7): p. 445-56.
36. Lee, Y.J., S.C. Jameson, and K.A. Hogquist, *Alternative memory in the CD8 T cell lineage.* Trends Immunol, 2011. **32**(2): p. 50-6.
37. Haluszczak, C., et al., *The antigen-specific CD8+ T cell repertoire in unimmunized mice includes memory phenotype cells bearing markers of homeostatic expansion.* J Exp Med, 2009. **206**(2): p. 435-48.
38. Huang, T., et al., *Commensal microbiota alter the abundance and TCR responsiveness of splenic naïve CD4+ T lymphocytes.* Clin Immunol, 2005. **117**(3): p. 221-30.
39. Lee, J.-Y., et al., *Virtual memory CD8 T cells display unique functional properties.* Proceedings of the National Academy of Sciences of the United States of America, 2013. **110**(33): p. 13498-13503.
40. White, J.T., et al., *Virtual memory T cells develop and mediate bystander protective immunity in an IL-15-dependent manner.* Nature Communications, 2016. **7**: p. 11291.

41. Pulko, V., et al., *Human memory T cells with a naive phenotype accumulate with aging and respond to persistent viruses.* Nature Immunology, 2016. **17**: p. 966.
42. Lee, J.-G., et al., *Identification of Human B-1 Helper T Cells With a Th1-Like Memory Phenotype and High Integrin CD49d Expression.* Frontiers in Immunology, 2018. **9**: p. 1617.
43. Gattinoni, L., et al., *A human memory T-cell subset with stem cell-like properties.* Nature medicine, 2011. **17**(10): p. 1290-1297.
44. Gattinoni, L., et al., *Wnt signaling arrests effector T cell differentiation and generates CD8+ memory stem cells.* Nature Medicine, 2009. **15**: p. 808.
45. Zhang, Y., et al., *Host-reactive CD8+ memory stem cells in graft-versus-host disease.* Nature Medicine, 2005. **11**(12): p. 1299-1305.
46. Kawabe, T., et al., *Memory-phenotype CD4(+) T cells spontaneously generated under steady state conditions exert innate Th1-like effector function.* Science immunology, 2017. **2**(12): p. eaam9304.
47. Sprent, J. and C.D. Surh, *Normal T cell homeostasis: the conversion of naïve cells into memory-phenotype cells.* Nature immunology, 2011. **12**(6): p. 478-484.
48. Sanos, S.L. and A. Diefenbach, *Isolation of NK Cells and NK-Like Cells from the Intestinal Lamina Propria*, in *Natural Killer Cell Protocols: Cellular and Molecular Methods*, K.S. Campbell, Editor. 2010, Humana Press: Totowa, NJ. p. 505-517.
49. Kim, D., et al., *TopHat2: accurate alignment of transcriptomes in the presence of insertions, deletions and gene fusions.* Genome Biol, 2013. **14**(4): p. R36.
50. Liao, Y., G.K. Smyth, and W. Shi, *featureCounts: an efficient general purpose program for assigning sequence reads to genomic features.* Bioinformatics, 2014. **30**(7): p. 923-30.
51. Love, M.I., W. Huber, and S. Anders, *Moderated estimation of fold change and dispersion for RNA-seq data with DESeq2.* Genome Biol, 2014. **15**(12): p. 550.
52. Korotkevich, G., V. Sukhov, and A. Sergushichev, *Fast gene set enrichment analysis.* bioRxiv, 2019: p. 060012.
53. Hu, G., et al., *Expression and regulation of intergenic long noncoding RNAs during T cell development and differentiation.* Nat Immunol, 2013. **14**(11): p. 1190-8.
54. Vahedi, G., et al., *STATs shape the active enhancer landscape of T cell populations.* Cell, 2012. **151**(5): p. 981-93.
55. Wei, G., et al., *Genome-wide analyses of transcription factor GATA3-mediated gene regulation in distinct T cell types.* Immunity, 2011. **35**(2): p. 299-311.
56. Tan, T.G., D. Mathis, and C. Benoist, *Singular role for T-BET(+)CXCR3(+) regulatory T cells in protection from autoimmune diabetes.* Proceedings of the National Academy of Sciences of the United States of America, 2016. **113**(49): p. 14103-14108.
57. Haluszczak, C., et al., *The antigen-specific CD8(+) T cell repertoire in unimmunized mice includes memory phenotype cells bearing markers of homeostatic expansion.* The Journal of Experimental Medicine, 2009. **206**(2): p. 435-448.
58. Parker, M.E. and M. Ciofani, *Regulation of γδ T Cell Effector Diversification in the Thymus.* Frontiers in immunology, 2020. **11**: p. 42-42.
59. Matsuda, J.L., et al., *T-bet concomitantly controls migration, survival, and effector functions during the development of Vα14i NKT cells.* Blood, 2006. **107**(7): p. 2797-2805.
60. Barros-Martins, J., et al., *Effector γδ T Cell Differentiation Relies on Master but Not Auxiliary Th Cell Transcription Factors.* The Journal of Immunology, 2016. **196**(9): p. 3642.
61. Townsend, M.J., et al., *T-bet Regulates the Terminal Maturation and Homeostasis of NK and Vα14i NKT Cells.* Immunity, 2004. **20**(4): p. 477-494.
62. Sumaria, N., et al., *Strong TCRγδ Signaling Prohibits Thymic Development of IL-17A-Secreting γδ T Cells.* Cell reports, 2017. **19**(12): p. 2469-2476.
63. Intlekofer, A.M., et al., *Effector and memory CD8+ T cell fate coupled by T-bet and eomesodermin.* Nature Immunology, 2005. **6**: p. 1236.

64. Klose, C.S.N., et al., *A T-bet gradient controls the fate and function of CCR6–RORγt+ innate lymphoid cells.* Nature, 2013. **494**: p. 261.
65. McPherson, R.C., et al., *T-bet Expression by Foxp3(+) T Regulatory Cells is Not Essential for Their Suppressive Function in CNS Autoimmune Disease or Colitis.* Frontiers in Immunology, 2015. **6**: p. 69.
66. Powell, N., et al., *The Transcription Factor T-bet Regulates Intestinal Inflammation Mediated by Interleukin-7 Receptor+ Innate Lymphoid Cells.* Immunity, 2012. **37**(4): p. 674-684.
67. Simonetta, F., A. Pradier, and E. Roosnek, *T-bet and Eomesodermin in NK Cell Development, Maturation, and Function.* Frontiers in Immunology, 2016. **7**: p. 241.
68. Wang, F., et al., *Regulatory role of NKG2D+ NK cells in intestinal lamina propria by secreting double-edged Th1 cytokines in ulcerative colitis.* Oncotarget, 2017. **8**(58): p. 98945-98952.
69. Artis, D. and H. Spits, *The biology of innate lymphoid cells.* Nature, 2015. **517**: p. 293.
70. Kedl, R.M. and M.F. Mescher, *Migration and activation of antigen-specific CD8+ T cells upon in vivo stimulation with allogeneic tumor.* The Journal of Immunology, 1997. **159**(2): p. 650.
71. Seder, R.A. and R. Ahmed, *Similarities and differences in CD4+ and CD8+ effector and memory T cell generation.* Nature Immunology, 2003. **4**: p. 835.
72. Groom, J.R. and A.D. Luster, *CXCR3 in T cell function.* Experimental cell research, 2011. **317**(5): p. 620-631.
73. Oghumu, S., et al., *Distinct Populations of Innate CD8⁺ T Cells Revealed in a CXCR3 Reporter Mouse.* The Journal of Immunology, 2013. **190**(5): p. 2229.
74. Tan, T.G., D. Mathis, and C. Benoist, *Singular role for T-BET^{+}CXCR3^{+} regulatory T cells in protection from autoimmune diabetes.* Proceedings of the National Academy of Sciences, 2016. **113**(49): p. 14103-14108.

Figure 1. T-bet fate mapping identifies a population of peripheral naïve-like CD4+ T cells that have experienced T-bet expression.

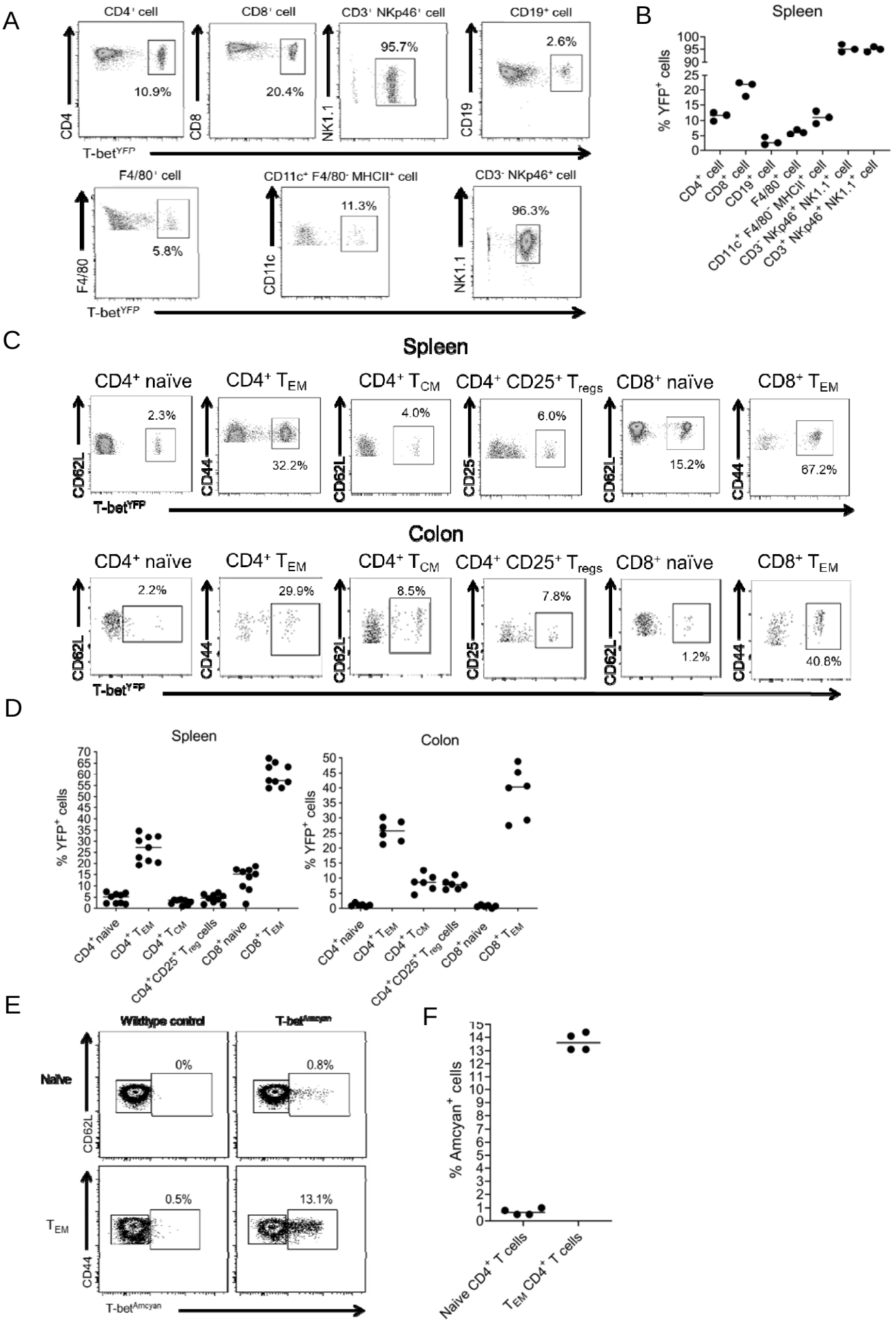

Figure 2 Naïve CD4+ T cells develop and exit the thymus without expressing T-bet.

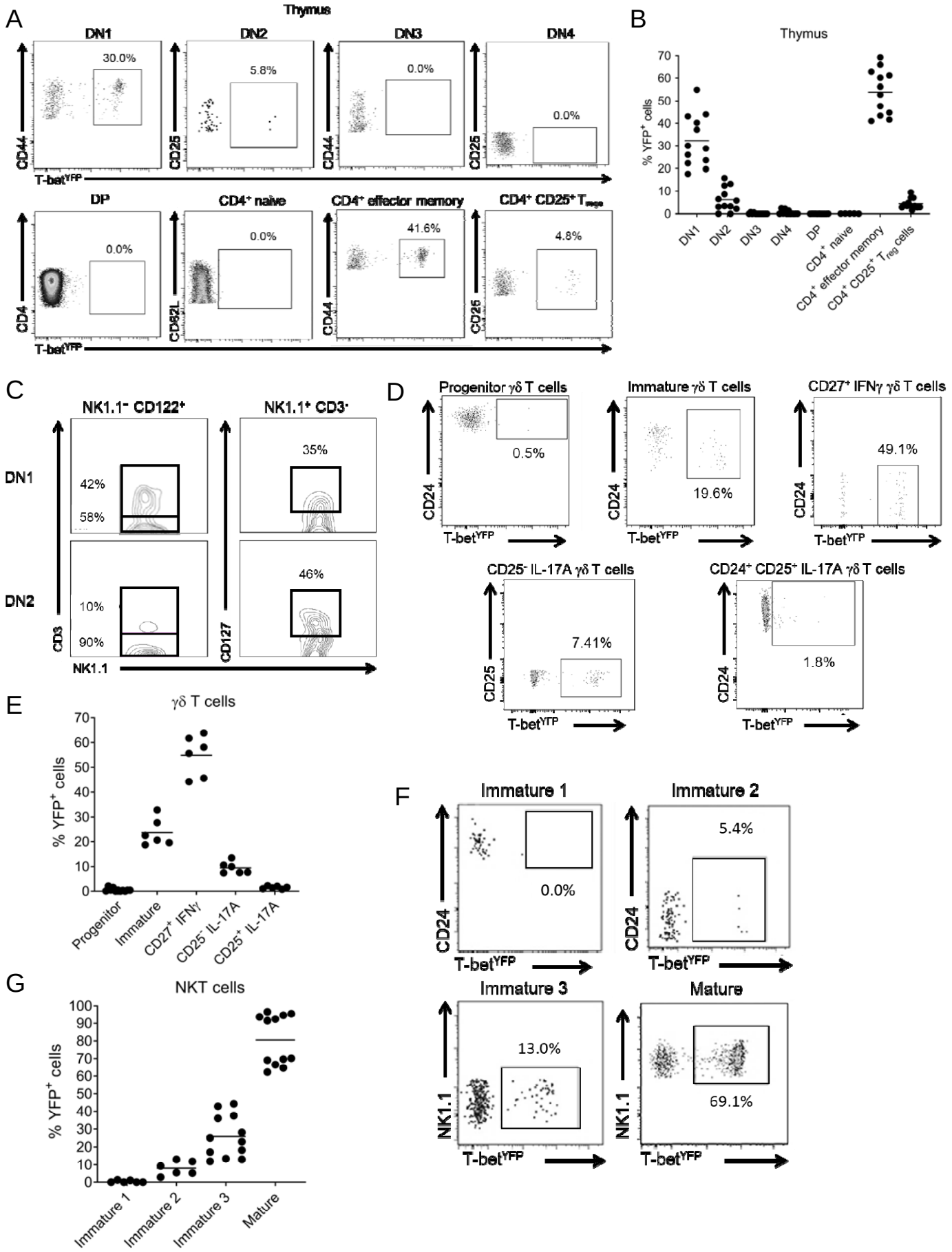

Figure 3. Naïve CD4+ T cells become YFP+ shortly after birth.

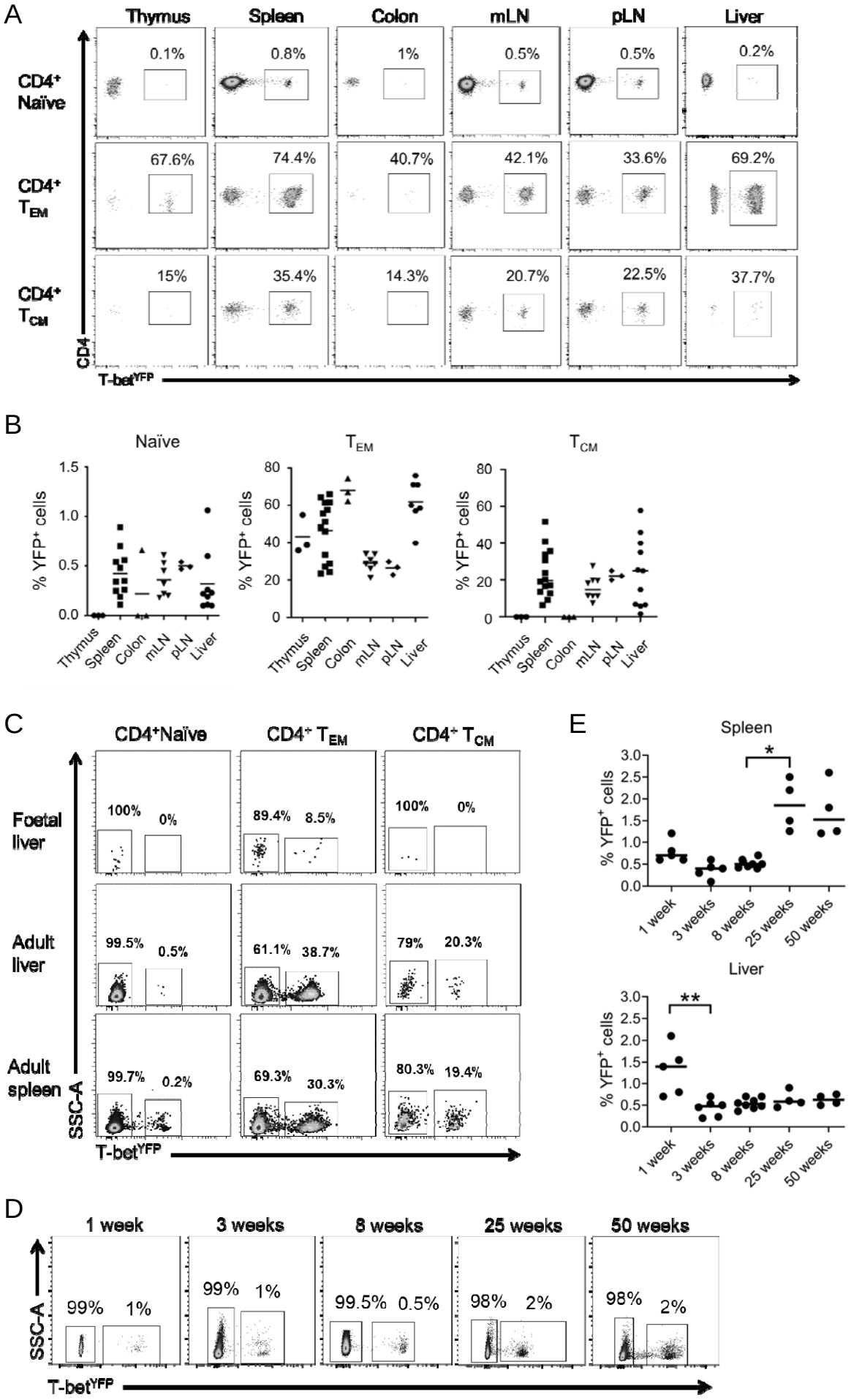

Figure 4. YFP$^+$ naïve-like cells do not correspond to previously defined CD4 T cell populations.

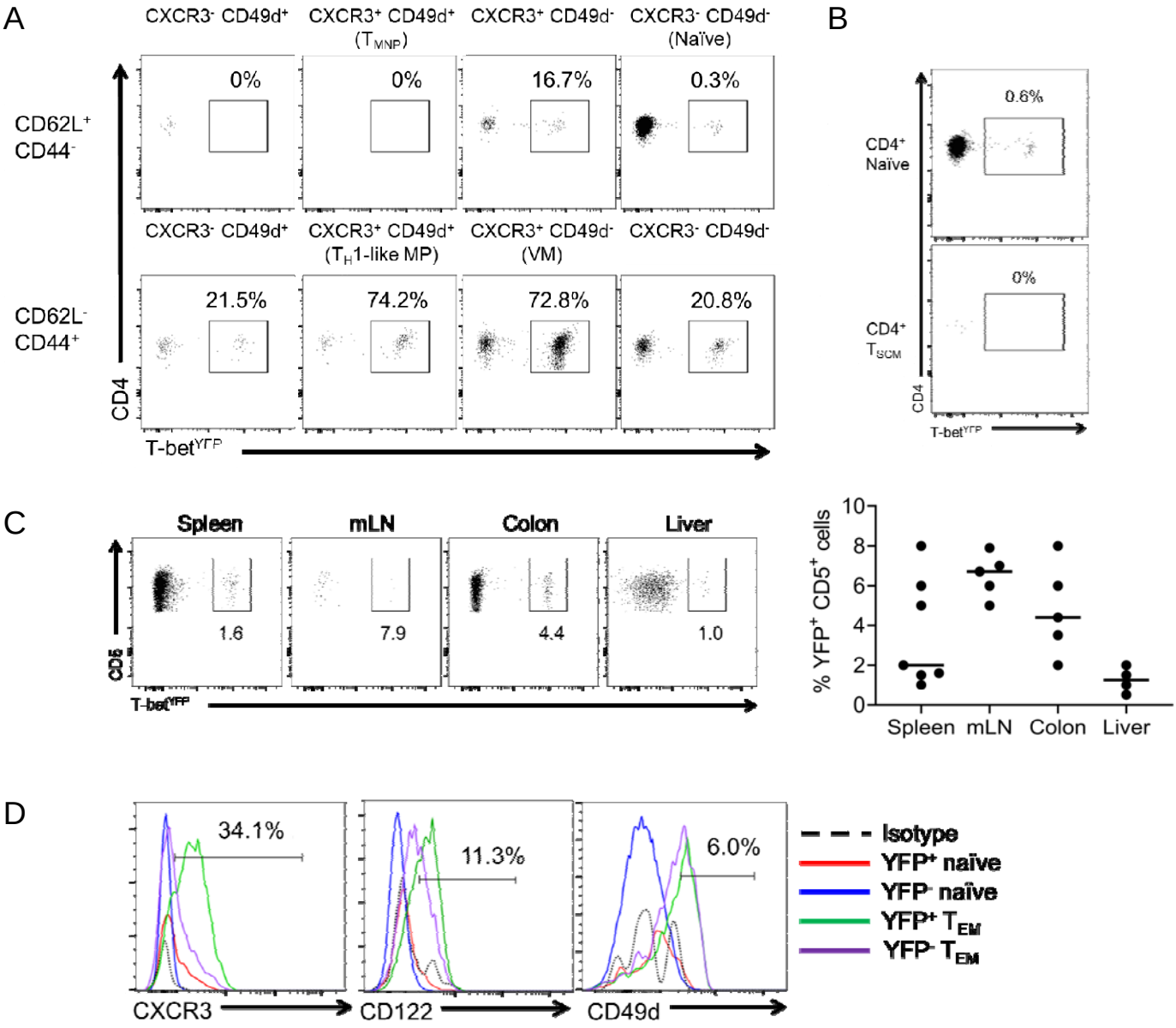

Figure 5. YFP⁺ naïve-like CD4⁺ T cells are polarised towards the T_H1 lineage.

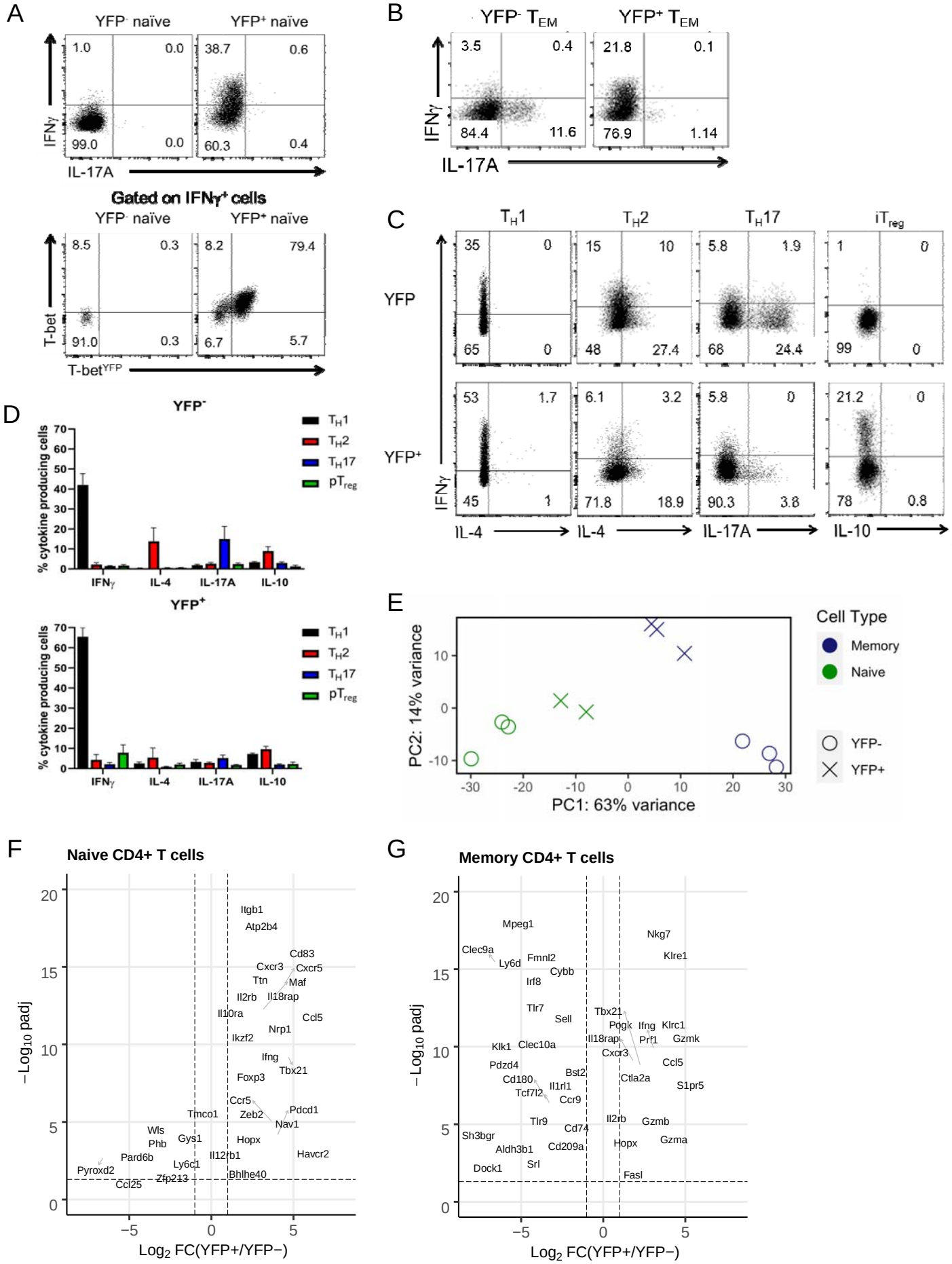
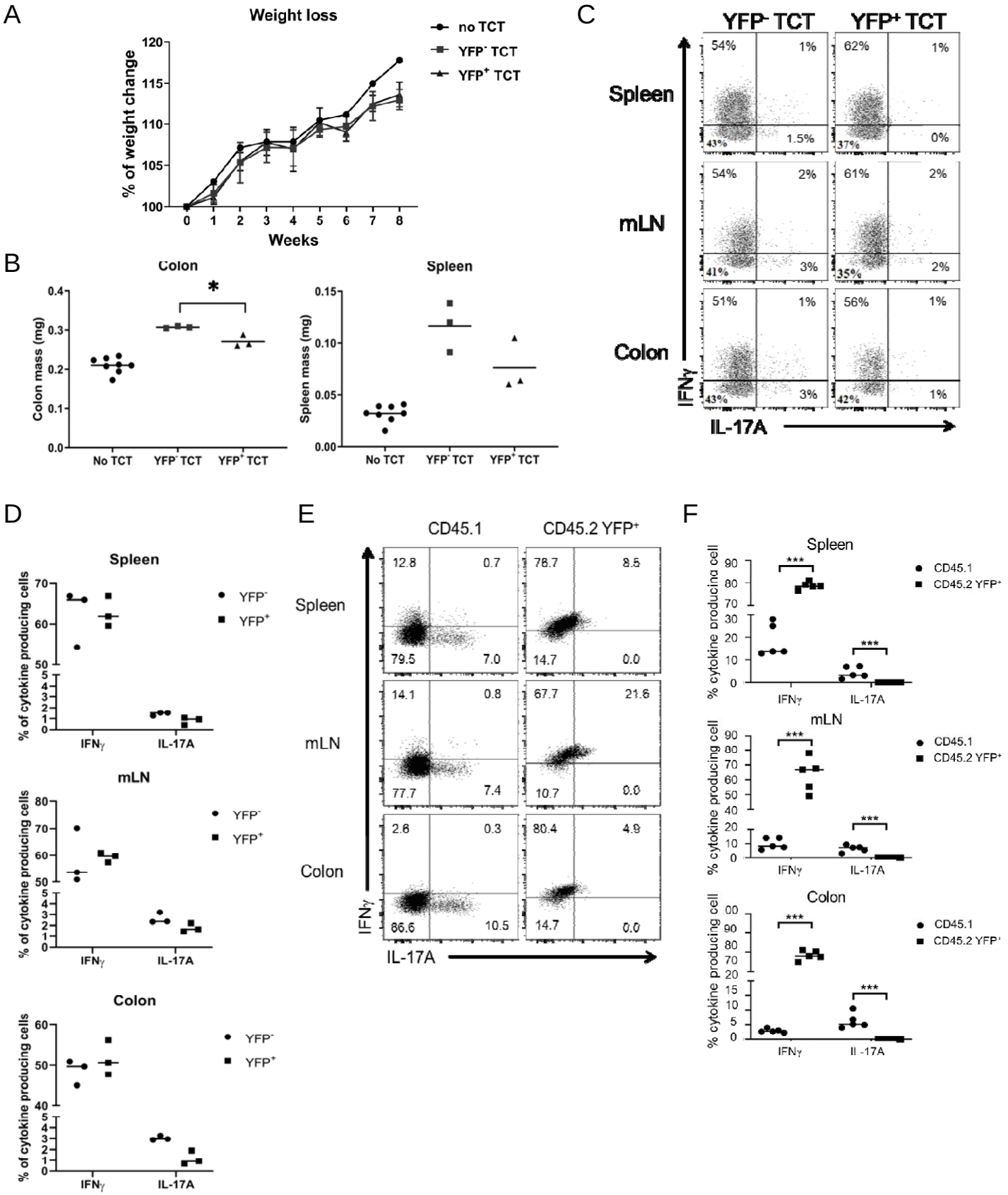
Figure 6. YFP$^+$ cells induce less inflammation but more IFNγ compared to conventional naïve CD4$^+$ T cells after transfer to *Rag2*$^{-/-}$ mice.